

BULETINUL INSTITUTULUI POLITEHNIC DIN IAȘI
Publicat de
Universitatea Tehnică „Gheorghe Asachi” din Iași
Tomul LXI (LXV), Fasc. 1, 2015
Secția
CONSTRUCȚII. ARHITECTURĂ

PLASTIC ANALYSIS OF COMPOSITE GIRDERS WITH CIRCULAR HOLES

BY

CĂTĂLIN MOGA and CRINA FENEȘAN*

Technical University of Cluj-Napoca
Faculty of Civil Engineering

Received: January 14, 2015

Accepted for publication: January 24, 2015

Abstract. In this paper some aspects concerning the design of steel-concrete composite rolled sections with circular holes in webs are presented. This paper presents the analysis of composite cellular girders that are part of a pedestrian bridge according to Eurocode 4 approach (SR EN 1994-1-1 and SR EN 1994-1-2).

The bending resistance moment is evaluated using the plastic design.

The design methodology is used in the design of footbridge superstructures.

Key words: composite girders; rolled sections with circular holes; footbridge superstructures; Euro codes; plastic design.

1. Introduction

Composite steel-concrete structures are applied on a large scale in civil engineering and in the erection of bridges due to their efficiency.

This paper presents the analysis of composite cellular girders that are part of a pedestrian bridge according to Eurocode 4 approach (SR EN 1994-1-1 and SR EN 1994-1-2).

*Corresponding author: *e-mail*: Crina.Fenesan@infra.utcluj.ro

The evaluation of the girder capable moment (resistance to bending) is made in the plastic behaviour field for the composite steel-concrete girder section.

Building phases. Characteristics and symbols

The following design sequences for composite girders have to be considered (Moga, 2014):

Phase 1: Construction stage

This building and structural behaviour phase occurs during the mounting of the main girders, until the reinforced concrete slab begins to act, that is after 28 days from the casting of the concrete.

Phase 1 includes the following loading stages (Moga, 2014):

- *Step 1:* after mounting the main girders.

During construction, the girder carries a uniformly distributed load, comprising its self-weight. At this stage, the top flange is laterally unrestrained and the girder are prone to lateral buckling.

- *Step 2:* after mounting the cross bars or the secondary girders, final bracings and possibly temporary bracings.

The girder support corresponding additional self-weights. Since cross girders or secondary beams provide lateral restraint to the compression flanges, the effective lateral buckling length can be taken as the length of the relevant segment between lateral restraint.

- *Step 3:* after casting the reinforced concrete slab (before setting).

The construction loading should be applied in addition to the self-weight of the girder, weight of wet concrete and weight of the decking.

Phase 2: Composite action

Subsequent loads are applied to the composite section:

- long term actions:
 - additional permanent weights added after the concrete gained adequate strength;
- short term loads:
 - live actions, wind actions, seismic action, pavements loads and other actions, if necessary.

2. The Plastic Resistance Moment

The plastic analysis can be applied to cross sections of Class 1 and Class 2.

In order to assess plastic moments, the following hypotheses are taken into consideration (Guţiu & Moga, 2014; SR EN 1994-1-1/2006; SR EN 1994-2/2006):

- a) total interaction between the metal girder and the concrete slab;
- b) the entire section of the metal slab is plastified (both the tensile and compressed area), the tensions in the steel are equal to the design resistance f_{yd} (equal to f_y/γ_{M0});
- c) the stresses in the compressed concrete have the ultimate value of $0.85 f_{cd} = 0.85 f_{ck}/\gamma_c$, constantly along the depth of the compressed area;
- d) in the flexible reinforcement from the reinforced concrete slab subjected to tension, stresses will be f_{sk}/γ_s ;
- e) the flexible reinforcement in the compressed slab can be neglected.

In Fig. 1 are presented the characteristic distributions of the stresses in the plastic design, according to EN 1994 (SR EN 1994-2/2006) of a fully connected composite girder, subjected to a positive, respectively negative bending moment.

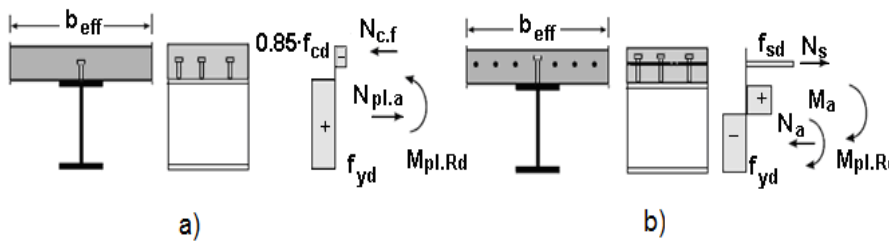


Fig. 1 – a – Positive bending moment; b – Negative bending moment.

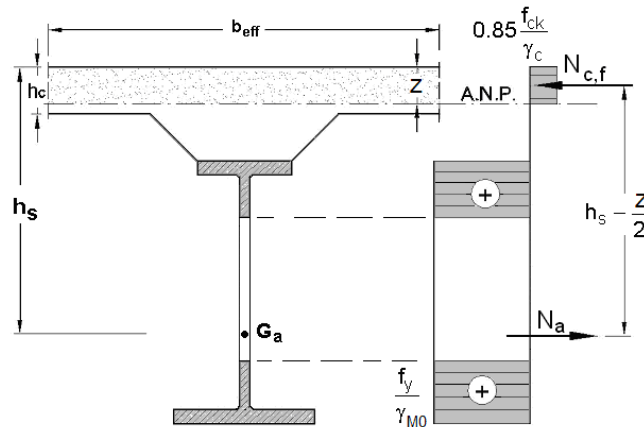


Fig. 2 – The neutral axis in the concrete slab.

In the case of a girder with circular holes subjected to a positive bending moment the stress distribution diagrams are presented in the Figs. 2 and 3.

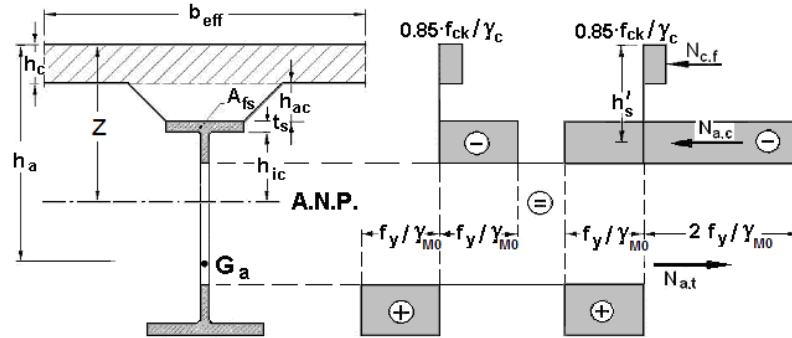


Fig. 3 – The neutral axis in the steel girder (hole zone).

3. Composite Steel-Concrete Footbridge. Non-Symmetrical Circular Hollow Steel Girders. Calculus in the Plastic Behaviour

The basic calculus of a deck with a composite steel-concrete girder for a pedestrian footbridge is presented starting from the following design data (Fig. 4) (Moga *et al.*, 2014):

a) structure span: $L = 24.0$ m; net width: $B_c = 3.00$ m;

b) the deck structure is made from two composite steel-concrete main girders, cross bars at the distance $l_a = 2.40$ m which are in connection with the cast-in-place reinforced concrete slab, Fig. 4;

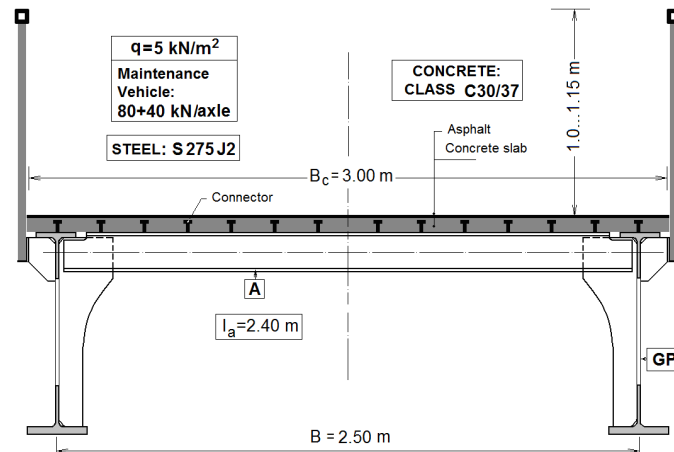


Fig. 4 – Cross section of the footbridge deck (Moga *et al.*, 2014).

c) the main steel girders are made from laminated profiles with circular holes in the web, produced by welding different rolled profiles for the two parts;

- d) the steel grade of the main girders: S 275 J2;
 e) the concrete in the monolith slab: Class 30/37.

The following notations shall be used: L – girder span; d_a – distance between cross bars or secondary girders; f_y – yield strength of steel; f_{ck} – the characteristic resistance to compression of the concrete; γ_M ; γ_c – partial safety coefficients for steel and concrete; $F1$; $F2$ – construction phases and of structural behaviour; lt ; st – long term load; short term load; A_{TS} – area of the top flange; A_{TI} – area of the bottom flange; $A_{TS}^{c.lt}$ – area of the composite top flange, evaluated at lt loads; $A_{TS}^{c.st}$ – area of the composite top flange, evaluated at st loads; h_0 – distance between the weight centres of the flanges for the steel girder; h_c^{lt} – distance between the weight centres of the flanges for the composite girder, lt loads; h_c^{st} – distance between the weight centres of the flanges for the composite girder, st loads; χ – reduction coefficient of the top flange buckling; M_{Ed} – general calculus bending moment; N_{Ed} – axial stress in the flanges, due to bending moment action.

Calculus data

Active slab width: $b_{eff} = 150 \text{ cm}$

Theoretical bending moment [3]

$$\text{Phase 1: } M_{Ed}^{F1} = 700 \text{ kNm}$$

$$\text{Phase 2: } M_{Ed}^{F2} = 982 \text{ kNm}$$

The main steel girders are built-up with circular holes in web arranged as follows (Fig. 5):

- upper part – IPE 600 rolled profile;
- lower part – HEB 800 rolled profile;
- hollows of diameter: $D = 640 \text{ mm}$;
- distance between hollow axes: $S = 960 \text{ mm}$;
- at the ends, the girder is built-up with web of variable depth.

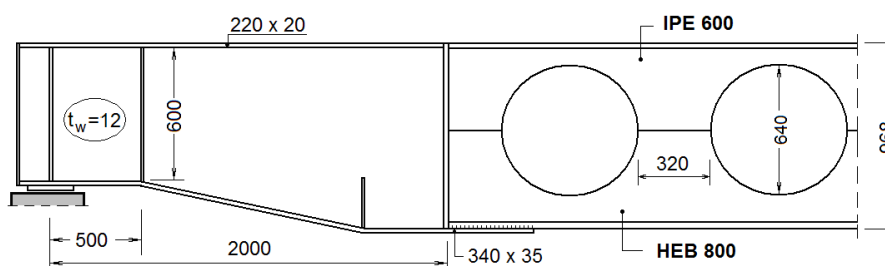


Fig. 5 – Steel girder with hollows (Moga *et al.*, 2014).

Let us take the hypothesis that in the hollow area the axial forces in the flanges is found from the M/h_0 ratio.

Phase 1: Construction stage

Characteristics of the flanges

In Fig. 6 are presented the strength characteristics of the top and bottom flange.

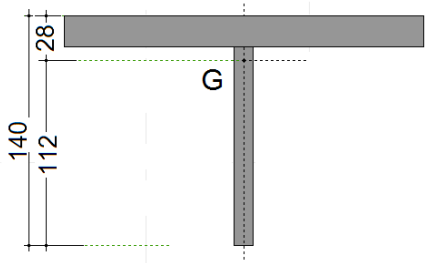
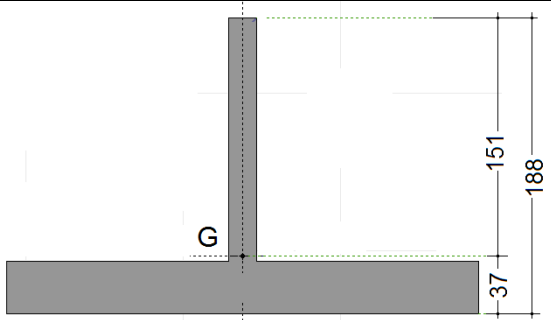
TOP FLANGE																															
	<table border="1"> <tr><td>$A_x[\text{cm}^2]$</td><td>=</td><td>56.32</td></tr> <tr><td>$I_y[\text{cm}^4]$</td><td>=</td><td>717.8</td></tr> <tr><td>$I_z[\text{cm}^4]$</td><td>=</td><td>1687.7</td></tr> <tr><td>$I_\omega[\text{cm}^6]$</td><td>=</td><td>595</td></tr> <tr><td>$W_{y,p}[\text{cm}^3]$</td><td>=</td><td>119.1</td></tr> <tr><td>$W_{z,p}[\text{cm}^3]$</td><td>=</td><td>234.3</td></tr> <tr><td>$W_{y,el,t}[\text{cm}^3]$</td><td>=</td><td>260.6</td></tr> <tr><td>$W_{y,el,b}[\text{cm}^3]$</td><td>=</td><td>63.8</td></tr> <tr><td>$W_{z,el,t}[\text{cm}^3]$</td><td>=</td><td>153.4</td></tr> <tr><td>$W_{z,el,b}[\text{cm}^3]$</td><td>=</td><td>153.4</td></tr> </table>	$A_x[\text{cm}^2]$	=	56.32	$I_y[\text{cm}^4]$	=	717.8	$I_z[\text{cm}^4]$	=	1687.7	$I_\omega[\text{cm}^6]$	=	595	$W_{y,p}[\text{cm}^3]$	=	119.1	$W_{z,p}[\text{cm}^3]$	=	234.3	$W_{y,el,t}[\text{cm}^3]$	=	260.6	$W_{y,el,b}[\text{cm}^3]$	=	63.8	$W_{z,el,t}[\text{cm}^3]$	=	153.4	$W_{z,el,b}[\text{cm}^3]$	=	153.4
$A_x[\text{cm}^2]$	=	56.32																													
$I_y[\text{cm}^4]$	=	717.8																													
$I_z[\text{cm}^4]$	=	1687.7																													
$I_\omega[\text{cm}^6]$	=	595																													
$W_{y,p}[\text{cm}^3]$	=	119.1																													
$W_{z,p}[\text{cm}^3]$	=	234.3																													
$W_{y,el,t}[\text{cm}^3]$	=	260.6																													
$W_{y,el,b}[\text{cm}^3]$	=	63.8																													
$W_{z,el,t}[\text{cm}^3]$	=	153.4																													
$W_{z,el,b}[\text{cm}^3]$	=	153.4																													
BOTTOM FLANGE																															
	<table border="1"> <tr><td>$A_x[\text{cm}^2]$</td><td>=</td><td>126.12</td></tr> <tr><td>$I_y[\text{cm}^4]$</td><td>=</td><td>2514.2</td></tr> <tr><td>$I_z[\text{cm}^4]$</td><td>=</td><td>7431.9</td></tr> <tr><td>$I_\omega[\text{cm}^6]$</td><td>=</td><td>7120</td></tr> <tr><td>$W_{y,p}[\text{cm}^3]$</td><td>=</td><td>330.5</td></tr> <tr><td>$W_{z,p}[\text{cm}^3]$</td><td>=</td><td>754.4</td></tr> <tr><td>$W_{y,el,t}[\text{cm}^3]$</td><td>=</td><td>166.2</td></tr> <tr><td>$W_{y,el,b}[\text{cm}^3]$</td><td>=</td><td>684.8</td></tr> <tr><td>$W_{z,el,t}[\text{cm}^3]$</td><td>=</td><td>495.5</td></tr> <tr><td>$W_{z,el,b}[\text{cm}^3]$</td><td>=</td><td>495.5</td></tr> </table>	$A_x[\text{cm}^2]$	=	126.12	$I_y[\text{cm}^4]$	=	2514.2	$I_z[\text{cm}^4]$	=	7431.9	$I_\omega[\text{cm}^6]$	=	7120	$W_{y,p}[\text{cm}^3]$	=	330.5	$W_{z,p}[\text{cm}^3]$	=	754.4	$W_{y,el,t}[\text{cm}^3]$	=	166.2	$W_{y,el,b}[\text{cm}^3]$	=	684.8	$W_{z,el,t}[\text{cm}^3]$	=	495.5	$W_{z,el,b}[\text{cm}^3]$	=	495.5
$A_x[\text{cm}^2]$	=	126.12																													
$I_y[\text{cm}^4]$	=	2514.2																													
$I_z[\text{cm}^4]$	=	7431.9																													
$I_\omega[\text{cm}^6]$	=	7120																													
$W_{y,p}[\text{cm}^3]$	=	330.5																													
$W_{z,p}[\text{cm}^3]$	=	754.4																													
$W_{y,el,t}[\text{cm}^3]$	=	166.2																													
$W_{y,el,b}[\text{cm}^3]$	=	684.8																													
$W_{z,el,t}[\text{cm}^3]$	=	495.5																													
$W_{z,el,b}[\text{cm}^3]$	=	495.5																													

Fig. 6 – Flanges characteristics.

The bending moment of the section is taken over through a couple of two equal and opposite sign forces, $C = -I$ (Fig. 7), where:

$$C = -I = N_{0,Ed}^{F1} = \frac{M_{Ed}^{F1}}{h_0}.$$

This verifies the condition: $N_{0,Ed}^{F1} / N_{b,Rd} \leq 1.0$.

The resistance to compression of the flange is that of a compressed bar of uniform section (SR EN 1993-1-1/2006).

$$N_{b.Rd} = \chi_{LT} \frac{A_f f_y}{\gamma_{M1}} \text{ – section Class 1, 2 or 3}$$

In general, the section of the flange is maximum Class 3 where we note the area of the compressed flange with A_0 , for simplification purpose.

$$\text{It yields: } N_{b.Rd} = \chi_{LT} \frac{A_0 f_y}{\gamma_{M1}}.$$

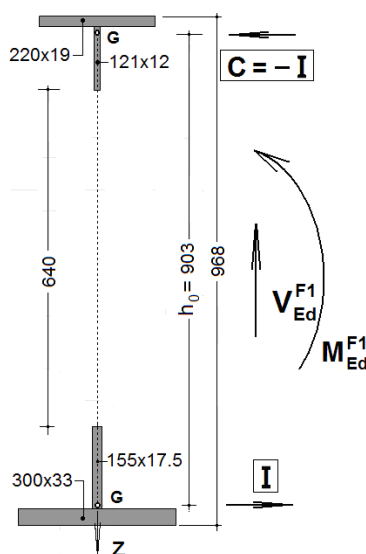


Fig. 7 – Cross section.

The reduction coefficient χ_{LT} takes into consideration that there is an opportunity to lose the compressed flange stability by lateral buckling during Phase 1; it is calculated in relation with the reduced slender coefficient $\bar{\lambda}$ (SR EN 1993-1-1/2006):

$$\bar{\lambda} = \bar{\lambda}_{LT} = \bar{\lambda}_{TF} = \sqrt{\frac{A_0 f_y}{N_{0.cr.TF}}} \Rightarrow \chi \text{ (curve d)}.$$

The critical force of stability loss is determined with relationship (Moga *et al.*, 2012):

$$N_{0.cr.TF} = \frac{I_{0.0}}{2(I_{0.y} + I_{0.z})} \left[(N_{0.cr.z} + N_{0.cr.T}) - \sqrt{(N_{0.cr.z} + N_{0.cr.T})^2 - 4 \frac{(I_{0.y} + I_{0.z})}{I_{0.0}} N_{0.cr.z} N_{0.cr.T}} \right]$$

where:

$$N_{0,cr,z} = \frac{\pi^2 EI_{0,z}}{L_{cr,z}^2}; I_{0,0} = I_{0,y} + I_{0,z} + A_0 z_s^2; N_{0,cr,T} = \frac{A_0}{I_{0,0}} \left(GI_{0,t} + \frac{\pi^2 EI_{0,\omega}}{L_{cr,T}^2} \right).$$

In the case under discussion, supposing measures are taken against losing stability until cross bars are fitted, the critical length will be equal to the distance between cross bars, namely: $L_{cr,z} = 2.40$ m.

It results:

$$I_{0,0} = I_{0,y} + I_{0,z} + A_0 z_s^2 = 717.8 + 1,687.7 + 56.32 \times 1.8^2 = 2,588 \text{ cm}^4;$$

$$I_{0,t} = \frac{1}{3} (22 \times 1.9^3 + 12.1 \times 1.2^3) = 57.3 \text{ cm}^4;$$

$$N_{0,cr,z} = \frac{\pi^2 EI_{0,z}}{L_{cr,z}^2} = \frac{\pi^2 \times 2.1 \times 10^6 \times 1,687.7}{240^2} = 0.607 \times 10^6 \text{ daN};$$

$$N_{0,cr,T} = \frac{A_0}{I_{0,0}} \left(GI_{0,t} + \frac{\pi^2 EI_{0,\omega}}{L_{cr,T}^2} \right) = \frac{56.32}{2,588} \left(0.81 \times 10^6 \times 57.3 + \frac{\pi^2 \times 2.1 \times 10^6 \times 595}{240^2} \right) = 1.01 \times 10^6 \text{ daN};$$

$$N_{0,cr,TF} = \frac{I_{0,0}}{2(I_{0,y} + I_{0,z})} \left[(N_{0,cr,z} + N_{0,cr,T}) - \sqrt{(N_{0,cr,z} + N_{0,cr,T})^2 - 4 \frac{(I_{0,y} + I_{0,z})}{I_{0,0}} N_{0,cr,z} N_{0,cr,T}} \right] =$$

$$= \frac{2,588}{2 \cdot 2405} \left[1.62 \cdot 10^6 - 10^6 \sqrt{1.62^2 - 4 \frac{2,405}{2,588} 0.607 \cdot 1.01} \right] = 0.55 \cdot 10^6 \text{ daN} = 5,500 \text{ kN};$$

$$\bar{\lambda}_{LT} = \sqrt{\frac{A_0 f_y}{N_{0,cr,TF}}} = \sqrt{\frac{56.32 \times 2,750}{0.55 \times 10^6}} = 0.53 \Rightarrow \chi_{LT} = 0.76.$$

In *Phase I*, the axial stresses in the flanges of the metal girder relative to the circular hollow middle are:

$$N_{0,Ed}^{F1} = \frac{M_{Ed}^{F1}}{h_0} = \frac{700}{0.903} = 775 \text{ kN}.$$

Taking into account the magnitude found for the reduction coefficient $\chi_{LT} = 0.76$, where one considers the loss of stability of the compressed flange by lateral – torsional buckling, the stresses in the metal girder flanges can be calculated:

a) in the top flange:

$$\sigma_{a.s}^{F1} = \frac{N_{0.Ed}^{F1}}{\chi_{LT} A_{TS}^{Otel}} = \frac{775 \times 10^2}{0.76 \times 56.32} = 1,811 \text{ daN/cm}^2;$$

b) in the bottom flange:

$$\sigma_{a.i}^{F1} = \frac{N_{0.Ed}^{F1}}{A_{Tl}} = \frac{775 \times 10^2}{126.12} = 614 \text{ daN/cm}^2.$$

Phase 2: Composite action

In *Phase 2* – of girder erection and behaviour, the steel girder acts together with the reinforced concrete slab through connectors.

Considering similar to *Phase 1*, that the two flanges are subjected to axial stresses, the bearing capacity of the girder is found when the plastic ultimate limit state is reached, respectively when the theoretical yield strength for steel and concrete is reached.

One should also consider that part of the bearing capacity of the steel flanges was used during *Phase 1*.

In composite steel-concrete girders, partial safety coefficients are used, namely $\gamma_{M0} = 1.0$ – for steel and $\gamma_c = 1.5$ – for concrete.

To assess the capable bending moment (*i.e.* the plastic resistance to bending) of the composite steel-concrete girder one makes use of the calculus diagram in Fig. 8.

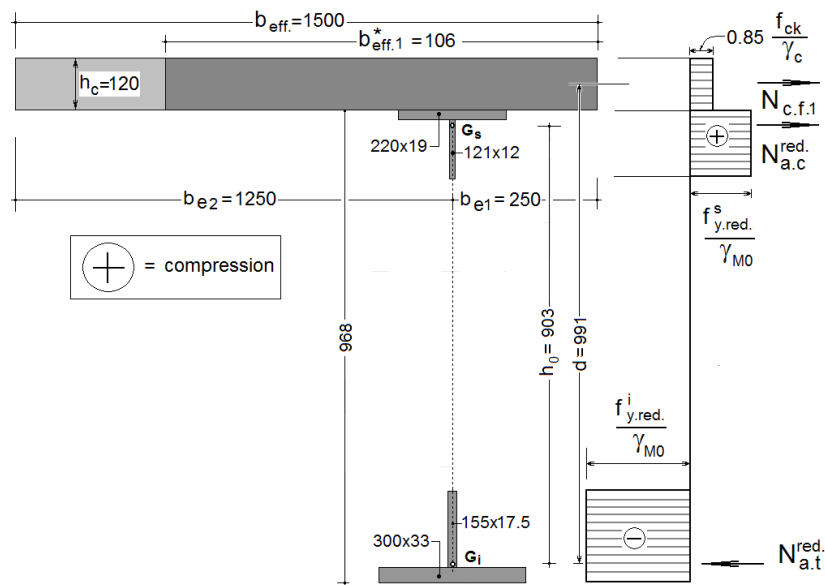


Fig. 8 – Stresses distribution on composite section.

The maximum normal stresses in the flanges of the steel girder are defined considering the tensions arising from the phase 1, as follows:

$$f_{y,\text{red.}}^s = f_y - \sigma_{a.s}^{F1} = 2,750 - 1,811 = 939 \text{ daN/cm}^2;$$

$$f_{yd}^s = \frac{f_{y,\text{red.}}^s}{\gamma_{M0}} = \frac{939}{1.0} = 939 \text{ daN/cm}^2;$$

$$f_{y,\text{red.}}^i = f_y - \sigma_{a.i}^{F1} = 2,750 - 614 = 2,136 \text{ daN/cm}^2;$$

$$f_{yd}^i = \frac{f_{y,\text{red.}}^i}{\gamma_{M0}} = \frac{2,136}{1.0} = 2,136 \text{ daN/cm}^2.$$

The resultants of the stresses (resultants of stress blocks) are:

$$N_{c.f.1} = A_{c.1} \times 0.85 \frac{f_{ck}}{\gamma_c} = 12 \times b_{\text{eff}.1}^* \times 0.85 \frac{300}{1.5} = 2,040 b_{\text{eff}.1}^* \text{ daN};$$

$$N_{a.c}^{\text{red.}} = A_{TS} f_{yd}^s = 56.32 \times 939 = 52,884 \text{ daN}.$$

The active width of the reinforced concrete slab is found from the projections of the resultants of stresses in the horizontal line:

$$N_{c.f.1} + N_{a.c}^{\text{red.}} = N_{a.t}^{\text{red.}} \Rightarrow b_{\text{eff}.1}^* \approx 106 \text{ cm} < b_{\text{eff}}; \quad N_{c.f.1} = 216,240 \text{ daN}.$$

The plastic bending moment resistance of the composite girder (the plastic resistance of the girder) can be found writing the moment of the resultant of the stresses (stress block) relative to the centre of the tensile stresses:

$$M_{\text{pl.Rd}}^{\text{red.}} = N_{c.f.1} d + N_{a.c}^{\text{red.}} h_0 = 2,162.4 \times 0.991 + 528.84 \times 0.903 = 2,620 \text{ kNm}.$$

It yields: $M_{Ed}^{F2} / M_{\text{pl.Rd}}^{\text{red.}} = 982 / 2,620 = 0.37 < 1$ (bending moment of Phase 2).

When the compressed flange is not in danger to lose the stability (buckling), the girder capable bending moment (i.e. the resistance to bending) can be assessed without reducing the steel yield strength (Fig. 9).

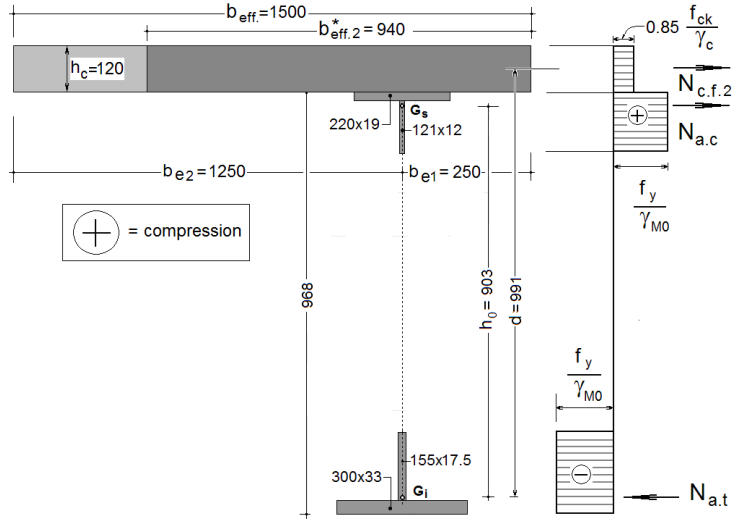


Fig. 9 – Stresses distribution on composite section.

The check relationship for this case refers to the total bending of the two Phases (F1+F2), namely:

$$\frac{M_{Ed}^{F1} + M_{Ed}^{F2}}{M_{pl.Rd}} \leq 1.$$

The following values are found:

$$N_{c.f.2} = A_{c.2} \cdot 0.85 \frac{f_{ck}}{\gamma_c} = 12b_{eff.2}^* \cdot 0.85 \frac{300}{1.5} = 2,040b_{eff.2}^* \text{ daN};$$

$$N_{a.c} = A_{TS} f_{yd} = 56.32 \times 2,750 = 154,880 \text{ daN};$$

$$N_{a.t} = A_{TI} f_{yd} = 126.12 \times 2,750 = 346,830 \text{ daN}.$$

The active width of the reinforced concrete slab can be found from the projections of the resultants of unit stresses in the horizontal line:

$$N_{c.f.2} + N_{a.c} = N_{a.t} \Rightarrow b_{eff.2}^* \approx 94 \text{ cm} < b_{eff}; \quad N_{c.f.2} = 191,760 \text{ daN}.$$

The plastic bending resistance of the girder shall be:

$$M_{pl.Rd} = N_{c.f.2} d + N_{a.c} h_0 = 1,917.6 \times 0.991 + 1,548.8 \times 0.903 = 3,299 \text{ kNm}.$$

$$\text{It yields: } \left(M_{Ed}^{F1} + M_{Ed}^{F2} \right) / M_{pl.Rd} = (700 + 982) / 3,299 = 0.51 < 1.$$

4. Remarks and Comments

Steel girders with circular holes with a symmetrical or non-symmetrical cross section (a more extended lower flange), structurally working together with a reinforced concrete slab, can be used to erect efficient structures that are efficient both from the cost viewpoint of civil and industrial buildings and from the viewpoint of crossing structures (pedestrian bridges, small span bridges, utility pipe crossing, etc.).

For the composite steel-concrete structures in use, the following aspects need to be mentioned:

a) in the initial formulations of EC4 Norm, on the calculus of composite steel-concrete structures, they used a partial safety coefficient for steel $\gamma_a = 1.10$, while in the final variant of the norm they use the coefficient $\gamma_{M0} = 1.0$;

b) a coefficient $\gamma_a = 1.10$ could be justified for a composite steel-concrete structure for the following reasons:

b₁) lack of structural homogeneity of the composite material (made up of steel, concrete and reinforcement);

b₂) the high global concrete safety coefficient, namely $\gamma_c / 0.85 = 1.50 / 0.85 = 1.76$, as compared to that of the steel – $\gamma_{M0} = 1.0$;

b₃) in the assessment of the capable bending moment (for the resistance to bending) in the plastic field of behaviour, according to E4, there is no explicit consideration of the partial consumption of the resistance of the metal girder during Phase 1 (when concrete and steel are not working together), respectively no consideration of the reduction coefficient χ_{LT} is taken.

c) in the case of girders with circular holes, it is recommended also to check the stresses at a certain distance from the hollow middle as the effect of the shear force can be significant.

The assessment of the girder bending resistance is made in the plastic behaviour field for the composite steel-concrete section.

The analysis in the plastic design can be applied to cross sections of Class 1 or Class 2 and can highlight the reserve of bearing capacity of the structure, as compared to the same analysis, but in the elastic design.

REFERENCES

- Guțiu I.Șt., Moga C., *Structuri compuse oțel-beton*. UTPRESS, 2014.
Moga P., *Pasarele pietonale metalice. Baza de calcul*. UTPRESS, 2014.

- Moga P., Gutiu I.Șt., Moga C., Danciu A., Suciu M., *Pasarele pietonale metalice. Manual de proiectare*. 2014
- Moga P., Guțiu Șt., Moga C., *Proiectarea elementelor din oțel. Teorie și aplicații*. U.T.PRESS, 2012.
- * * Eurocod 3: *Proiectarea structurilor de oțel*. Partea 1-1: *Reguli generale și reguli pentru clădiri*. SR EN 1993-1-1/2006.
- * * Eurocod 4: *Proiectarea structurilor compozite de oțel și beton*. Partea 1-1 : *Reguli generale și reguli pentru clădiri*. SR EN 1994-1- 1/2006.
- * * Eurocod 4: *Proiectarea structurilor compozite de oțel și beton*. Partea 2: *Reguli generale și reguli pentru poduri*. SR EN 1994-2/2006.

CALCULUL PLASTIC AL GRINZILOR COMPOZITE CU GOLURI CIRCULARE

(Rezumat)

Se prezintă o adaptare a metodologiei de calcul a grinzilor compuse oțel-beton prezentată în euro-normele *SR EN 1994-1-1: 2006: Eurocod 4: Proiectarea structurilor compozite de oțel și beton. Partea 1-1: Reguli generale și reguli pentru clădiri* și *SR EN 1994-2: 2006: Eurocod 4: Proiectarea structurilor compozite de oțel și beton. Partea 2: Reguli generale și reguli pentru poduri*, la calculul grinzilor cu goluri compozite, pentru o pasarelă pietonală.

Evaluarea momentului capabil al grinzii (rezistența la încovoiere) se face în domeniul de comportare plastică a secțiunii compuse oțel-beton.

